

# Modeling and Control of port dynamics of a tilt-rotor quadcopter

Nikhilraj A\* Harsha Simha\*\* H Priyadarshan\*\*\*

\* *Indian Institute of Space Science and Technology, Trivandrum, (e-mail: nikhilraja.15@res.iist.ac.in)*

\*\* *Indian Institute of Space Science and Technology, Trivandrum, (e-mail: harshasimhams@iist.ac.in)*

\*\*\* *Indian Institute of Space Science and Technology, Trivandrum, (e-mail: priyadarshnam@iist.ac.in)*

**Abstract:** Tilt-rotor quadcopters can effectively decouple translational and rotational dynamics, which makes them suitable candidates for aerial manipulation tasks. This is achieved by tilting the individual propellers to generate forces in any direction with respect to its body frame. This paper addresses the port trajectory tracking of a tilt-rotor quadcopter while following an independent attitude profile. We propose a sliding mode controller for the trajectory tracking of a rigid port mounted on the tilt-rotor quadcopter. Attitude is represented using rotation matrices to ensure global representation. We illustrate simultaneous tracking of port and attitude profiles numerically.

Copyright © 2022 The Authors. This is an open access article under the CC BY-NC-ND license (<https://creativecommons.org/licenses/by-nc-nd/4.0/>)

*Keywords:* quadrotors, sliding mode control.

## 1. INTRODUCTION

For the last two decades, quadrotors have been gaining popularity in aerial robotics because of their superior agility and disturbance rejection capabilities. The surge in use of such systems kindled the development of quadrotors with advanced capabilities compared to the traditional ones. A relatively new player in this field is tilt-rotor quadcopter. Tilt-rotors have considerable advantages over traditional quadrotors in terms of agility and maneuverability.

A traditional quadrotor is underactuated, and as a result, the translational dynamics depends on the instantaneous attitude. The traditional quadrotors cannot hover in a tilted position or simultaneously satisfy both translational and rotational requirements. While tracking a desired trajectory, quadrotors change their attitude and consequently alter the view of the onboard surveillance camera, which has a detrimental impact on vision-based applications. On the other hand, tilt-rotor quadcopters, overactuated by design, are not confined by these limitations. Tilt-rotors overcome these shortcomings by employing tilt-able propellers. This versatility enables the tilt-rotor quadcopters to generate forces in any direction and effectively decouple translational and rotational dynamics under normal flight conditions.

In this paper, we exploit the capability of the tilt-rotor quadcopter to track a translational trajectory for a given attitude profile and propose a trajectory tracking controller for port position and port velocity. The control of a port or a manipulator mounted on an airborne device

has many applications in aerial robotics. It can be used for tool operations, grasping, and aerial manipulation.

Though not studied as extensively as traditional quadrotors, tilt-rotor quadcopter design and control techniques have piqued numerous academics' interest in the last decade. In Ryll et al. (2012), the dynamic model of a tilt-rotor quadcopter is derived. This work also discusses the controllability property and designs a trajectory tracking controller for the tilt-rotor. Various control schemes such as inverse dynamics based control Falconi and Melchiorri (2012), feedback linearization control Nemati and Kumar (2014), LQR control Willis et al. (2020), PD sliding mode control Alkamachi and Erçelebi (2019) are designed for trajectory tracking control of tilt-rotor quadcopters. In Kumar et al. (2017), feed-forward control for tracking of aggressive trajectories is presented. A geometric controller is described in Invernizzi and Lovera (2017) for trajectory tracking on SE(3), considering the constraints on the applied force. Albeit the control of translational dynamics has been analyzed comprehensively, the control of a rigid tool or manipulator mounted on the tilt-rotor quadcopter is a field less explored.

Unlike tilt-rotors, traditional quadrotors have been abundantly used for aerial manipulation. In Yang and Lee (2014) and Martin et al. (2013), trajectory tracking control of the manipulator end effector has been discussed. A rigid tool attached to the quadrotor is more challenging but for a specific set of applications such as screw operations, control of such rigid tools is of extreme significance. The modeling and trajectory tracking control of quadrotors for tool operations have been performed for a variety of uses by Nguyen and Lee (2013) and Nguyen et al. (2015). Contrary to the traditional quadrotors, tilt-rotor's adeptness

\* The authors are with the Department of Avionics, Indian Institute of Space Science and Technology, DoS, Government of India, Thiruvananthapuram 695547, India (e-mail: nikhilraja.15@res.iist.ac.in).

in decoupling translation from rotation makes them the ideal candidates for similar applications.

In this paper, we design a trajectory tracking scheme for position and velocity of a port mounted on the tilt-rotor quadcopter. According to the author's best knowledge, there has not been any studies focusing on the control of port position and velocity of a tilt-rotor quadcopter so far. We propose a controller for the port trajectory tracking. We demonstrate that port trajectory can be tracked independent of the attitude profile.

Since rotation matrix presents a global and unique form of attitude representation Chaturvedi et al. (2011), we use it to define the quadrotor's attitude.

The paper is divided into four sections. In section 2, we introduce the basics and present the mathematical model of the tilt-rotors employing rotation matrices for attitude representation. We design a sliding mode controller for the position and velocity tracking of the tilt-rotor port in Section 3, and prove its stability. Section 4 includes illustration of complex trajectory tracking capabilities using numerical simulations.

## 2. EQUATIONS OF MOTION OF TILT-ROTOR QUADCOPTER

We consider a tilt rotor quadrotor as illustrated in Fig. 1. An actuator pivot joint allows the arm of the propeller to rotate and deliver a net force with respect to tilt-rotor quadcopter's body frame. The angle of tilt of  $i^{th}$  propeller is represented using  $\theta_i$  whereas the thrust force generated perpendicular to the plane of  $i^{th}$  propeller is denoted as  $f_i \in \mathbb{R}$ . Similarly, the moment produced by the propeller  $i$ , is represented as  $M_i$ . The tilt angle  $\theta_i$  and the thrust force  $f_i$  are the eight inputs of the tilt-rotor, which makes it an overactuated system. We define three reference frames - an

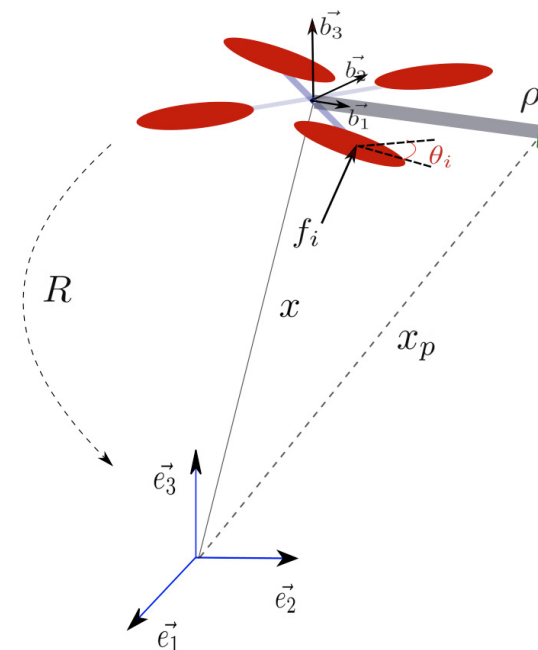


Fig. 1. Tilt-rotor model

inertial frame, a body fixed frame, and a frame fixed on the arm of each of the four propellers - to define the dynamic model of the tilt-rotor quadcopter.  $R$  is the rotation matrix from body frame to inertial frame and  $R_i$  the rotation matrix from the  $i^{th}$  propeller arm frame to the body fixed frame.  $J$  and  $m$  are respectively the moment of inertia and mass of the tilt-rotor. The port is mounted as shown in Fig. 1.  $\rho$  is the position vector of the port expressed in body fixed frame.

The individual propeller forces generate a net thrust  $f \in \mathbb{R}^3$  expressed in tilt-rotor quadcopter's body frame as,

$$f = \sum_{i=1}^4 R_i^p(\theta_i) f_i e_3, \quad (1)$$

where rotation matrix  $R_i^p$  is a function of the tilt angle  $\theta_i$  of the  $i^{th}$  propeller and  $e_3 = [0 \ 0 \ 1]^T$ . For example, this rotation matrix for a propeller mounted on the pitch axis of the tilt-rotor's body frame and is tilted counter-clockwise by an angle  $\theta$  is given as,

$$\begin{bmatrix} \cos(\theta) & 0 & \sin(\theta) \\ 0 & 1 & 0 \\ -\sin(\theta) & 0 & \cos(\theta) \end{bmatrix}.$$

Both the forces and moments of individual propellers generate a net moment,  $M \in \mathbb{R}^3$ , with respect to the body-fixed frame which is expressed as follows.

$$M = \sum_{i=1}^4 \alpha_i R_i^p(\theta_i) M_i e_3 + \sum_{i=1}^4 l_i \times (R_i^p(\theta_i) f_i e_3), \quad (2)$$

where  $l_i \in \mathbb{R}^3$  is the position vector of the  $i^{th}$  propeller arm expressed in body frame and  $\alpha_i = \pm 1$  is determined by the direction of angular velocity of  $i^{th}$  propeller. We define,  $x \in \mathbb{R}^3$  the position of centre of mass of the tilt-rotor quadcopter in inertial frame,  $v \in \mathbb{R}^3$  the velocity in inertial frame, and  $\Omega \in \mathbb{R}^3$  the angular velocity in the body-fixed frame. The equations of motion of the tilt-rotor quadcopter can be derived as,

$$\dot{x} = v \quad (3)$$

$$m\ddot{x} = -mge_3 + R \left( \sum_{i=1}^4 R_i^p(\theta_i) f_i e_3 \right) \quad (4)$$

$$\begin{aligned} J\dot{\Omega} &= \left( \sum_{i=1}^4 \alpha_i R_i^p(\theta_i) M_i e_3 \right) - \Omega \times J\Omega \\ &+ \left( \sum_{i=1}^4 l_i \times (R_i^p(\theta_i) f_i e_3) \right) \end{aligned} \quad (5)$$

$$\dot{R} = R\hat{\Omega}, \quad (6)$$

We can simplify the dynamics by considering only the net force and moment instead of individual propeller forces which yields the dynamics of the tilt-rotor quadcopter represented by equations (7)-(10). We will use the mapping defined in equation (11) (refer the footnote of the next page) later to compute individual propeller forces and tilt angles from the net force and moment.

$$\dot{x} = v \quad (7)$$

$$m\ddot{x} = -mge_3 + Rf \quad (8)$$

$$J\dot{\Omega} = M - \Omega \times J\Omega \quad (9)$$

$$\dot{R} = R\hat{\Omega}. \quad (10)$$

where the hat operator,  $(\hat{\cdot}) : \mathbb{R}^3 \rightarrow \mathfrak{so}(3)$  for  $y = [y_1, y_2, y_3]^T$  is,

$$\hat{y} = \begin{bmatrix} 0 & -y_3 & y_2 \\ y_3 & 0 & -y_1 \\ -y_2 & y_1 & 0 \end{bmatrix}.$$

Here, we consider a tilt-rotor with single axis tilt  $\theta_i \in \mathbb{R}$ . The net force and moment can be effectively mapped on to the individual propeller forces and tilt-angles using the mapping defined in equation (11).

In this paper, we use the simplified model of tilt-rotor quadcopter for the controller design since the mapping represented in equation (11) is invertible except when at least one of the propellers stops functioning Invernizzi and Lovera (2017). That is, under normal flight conditions, any net force and moment can be mapped into corresponding propeller thrusts and tilt angles by computing the pseudo inverse of the matrix given in (11).

Now that we have developed the equations of motion, we will derive the port dynamics of the tilt-rotor in the next subsection.

### 2.1 Modeling of port dynamics

The port position in inertial frame  $x_p$  can be written as,

$$x_p = x + R\rho. \quad (12)$$

The port dynamics is obtained by differentiating the above equation with respect to time.

$$\dot{x}_p = v + R\hat{\Omega}\rho \quad (13)$$

$$\begin{aligned} \ddot{x}_p &= \dot{v}_p = \ddot{x} + R\hat{\Omega}\hat{\Omega}\rho + R\dot{\hat{\Omega}}\rho \\ \ddot{x}_p &= -ge_3 + \frac{Rf}{m} + R\hat{\Omega}\hat{\Omega}\rho + R\dot{\hat{\Omega}}\rho, \end{aligned} \quad (14)$$

where  $v_p$  is the port velocity expressed in inertial frame.

It is evident from equation (14) that port dynamics depend on the angular velocity and instantaneous attitude. However, for a given attitude profile, we can use the above set of equations to develop a controller for the port trajectory tracking. The proposed control scheme, in detail, along with the proof of its stability is given in the next subsection.

## 3. TRAJECTORY TRACKING CONTROL OF PORT POSITION AND VELOCITY

In this section, first we design a sliding mode controller which ensures that trajectory tracking errors converges to zero. In the subsequent subsection we discuss the attitude controller adopted for the tilt-rotor quadcopter.

### 3.1 Control law design for the port dynamics of tilt-rotor quadcopter

Let us start by defining the port position error,  $e_{x_p}$  and velocity error  $\dot{e}_{x_p} = e_{v_p}$  as,  $e_{x_p} = x_p - x_p^d$  and  $e_{v_p} = v_p - v_p^d$ .  $x_p^d$  and  $v_p^d$  are the desired port position and velocity respectively.

*Theorem 1.* For the tilt-rotor port dynamics represented by the equations (3)-(6) and (14), the port trajectory tracking error will converge to zero using the control law,

$$f = mR^T \left( -\text{sign}(\sigma) - ke_{v_p} + ge_3 - R\hat{\Omega}\hat{\Omega}\rho - R\dot{\hat{\Omega}}\rho + \dot{v}_p^d \right), \quad (15)$$

where  $\text{sign}(\sigma) = [\text{sign}(\sigma_1) \text{sign}(\sigma_2) \text{sign}(\sigma_3)]^T$  for the sliding surface  $\sigma$  defined in equation (16).

**Proof.** Let us define the sliding surface as,

$$\sigma = k_v e_{x_p} + \dot{e}_{x_p}, \quad (16)$$

The following Lyapunov function  $V$  is opted.

$$V = \frac{1}{2} \sigma^T \sigma$$

The time derivative of Lyapunov function is obtained as,

$$\dot{V} = \sigma^T \dot{\sigma}. \quad (17)$$

We obtain the expression for  $\dot{\sigma}$  by taking the time derivative of the equation (16).

$$\dot{\sigma} = k_v (\dot{x}_p - \dot{x}_p^d) + (\dot{v}_p - \dot{v}_p^d)$$

After substituting for  $\dot{v}_p$ , we obtain,

$$\dot{\sigma} = k_v (v_p - v_p^d) + (-ge_3 + \frac{Rf}{m} + R\hat{\Omega}\hat{\Omega}\rho + R\dot{\hat{\Omega}}\rho) - \dot{v}_p^d.$$

Once we substitute the expression for  $\dot{\sigma}$  in equation (17) we obtain,

$$\dot{V} = \sigma^T \left( k_v e_{v_p} + (-ge_3 + \frac{Rf}{m} + R\hat{\Omega}\hat{\Omega}\rho + R\dot{\hat{\Omega}}\rho) - \dot{v}_p^d \right) \quad (18)$$

We choose the control force  $f = mR^T (-k_v e_{v_p} + ge_3 - \text{sign}(\sigma) - R\hat{\Omega}\hat{\Omega}\rho - R\dot{\hat{\Omega}}\rho + \dot{v}_p^d)$ . The above equation can be rewritten as,

$$\dot{V} = -\sigma^T \text{sign}(\sigma) < 0.$$

To eliminate chattering, we modify the designed controller of equation (15) by employing a sigmoid function instead of a sign function.

We have designed a controller to track the port trajectory. However, the desired control force is dependent on the rotational dynamics. In the next subsection, we discuss the attitude controller employed for the attitude subsystem.

### 3.2 Attitude Subsystem

A desired attitude profile  $R_d \in SO(3)$  is given. Corresponding angular velocity command is  $\hat{\Omega}_d = R_d^T \dot{R}_d$ . We use an attitude error  $e_R = \frac{1}{2}(R_d^T R - R^T R_d)^\vee$  derived from the standard attitude error function  $\psi(R, R_d) = \frac{1}{2} \text{tr}(I - R_d^T R)$ . The angular velocity error, expressed in body fixed frame is chosen as  $e_\Omega = \Omega - R^T R_d \hat{\Omega}_d$ . We use a non-linear geometric controller based on Lee et al. (2010), expressed as,

$$M = -K_R e_R - K_\Omega e_\Omega + \Omega \times J \Omega - J(\hat{\Omega} R^T R_d \hat{\Omega}_d - R^T R_d \hat{\Omega}_d). \quad (19)$$

The details of the implementation of the proposed control scheme is illustrated in Fig. 2. The attitude error function  $\psi$  has three critical points other than the desired equilibrium which is  $R = R_d$ . The additional critical points are  $R_d \exp(\pi \hat{e}_i)$  where  $i = 1, 2, 3$ . The corresponding upper bound is 2, that is, the attitude error function corresponding to initial attitude error should be less than

2. This upper bound can be extended using an attitude error function  $\psi = \frac{1}{2}tr(G(I - R_d^T R))$  where  $G$  is a diagonal matrix.

We have described the control techniques employed for the trajectory tracking of tilt-rotor port in this section. We demonstrate the tracking of port trajectory for a give attitude profile in the next section using numerical simulations.

#### 4. NUMERICAL STUDIES

For the numerical simulations we use the geometrically accurate discretized model similar to the one proposed in Nikhilraj et al. (2019). Since the proposed controller is dependent on the rotational dynamics, we set the frequency of the attitude control loop higher than the port control loop for the proper functioning of the proposed controller. The designed control scheme is applied to the model and the resulting plots are shown in figures 3-6.

Consider a quadrotor of mass  $2kg$  having a moment of inertia  $diag(0.07928, 0.0752, 0.1226)kgm^2$ . The position vector of the port,  $\rho$ , expressed in body fixed frame is chosen as  $[0.5 \ 0 \ 0]^T$ .

The control parameters used for both simulations are,  $\mu = 10, k_p = 22, k_R = 8.8, k_\Omega = 4$

We study two complex flight maneuvers with both port dynamics and attitude requirements. Details of the desired trajectories are given below.

Case 1: Track a lemniscate while satisfying a constantly varying yaw requirement.

$$x_p^d = \left[ \frac{acos(t)}{1 + sin^2(t)} \quad \frac{asin(t)cos(t)}{1 + sin^2(t)} \quad 0 \right]^T$$

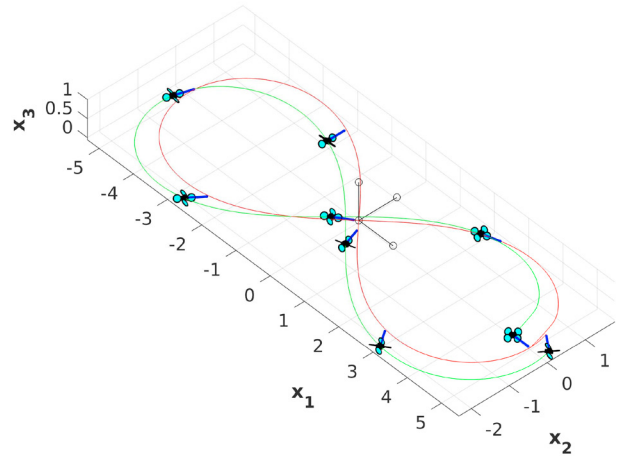


Fig. 3. Case 1: Port Trajectory

$$R_d = exp([0 \ 0 \ \frac{\pi}{8} t]^\wedge)$$

Initial conditions are as follows.

$$x = [3 \ 0 \ 0]^T, \quad R = I_{3 \times 3}$$

Case 2: Simultaneously track a port trajectory varying along all three axes and an attitude with varying roll and yaw requirements.

$$x_p^d = [1 + 0.5t \ 0.2t \ 0.2sin(\pi t)]^T$$

$$R_d = exp([0 \ 0.5\pi(t - 8) \ \frac{\pi}{12} t]^\wedge)$$

Initial conditions are chosen as,

$$x = [0 \ 0 \ 0]^T \quad R = I_{3 \times 3}$$

$$\begin{bmatrix} f \\ M \end{bmatrix} = \begin{bmatrix} 0 & 0 & 0 & 0 & 0 & -1 & 0 & -1 \\ 0 & 0 & 0 & 0 & 1 & 0 & 1 & 0 \\ 1 & 1 & 1 & 1 & 0 & 0 & 0 & 0 \\ 0 & L & 0 & -L & 0 & \alpha_2 \frac{k_f}{k_m} & 0 & \alpha_4 \frac{k_f}{k_m} \\ L & 0 & -L & 0 & -\alpha_1 \frac{k_f}{k_m} & 0 & -\alpha_3 \frac{k_f}{k_m} & 0 \\ -\alpha_1 \frac{k_f}{k_m} & -\alpha_2 \frac{k_f}{k_m} & -\alpha_3 \frac{k_f}{k_m} & -\alpha_4 \frac{k_f}{k_m} & L & L & L & L \end{bmatrix} \begin{bmatrix} f_1 sin\theta_1 \\ f_2 sin\theta_2 \\ f_3 sin\theta_3 \\ f_4 sin\theta_4 \\ f_1 cos\theta_1 \\ f_2 cos\theta_2 \\ f_3 cos\theta_3 \\ f_4 cos\theta_4 \end{bmatrix}, \quad (11)$$

where  $k_f$  and  $k_m$  are the force and torque constants of the propeller motor and  $L \in \mathbb{R}$  is the length of the propeller arm.

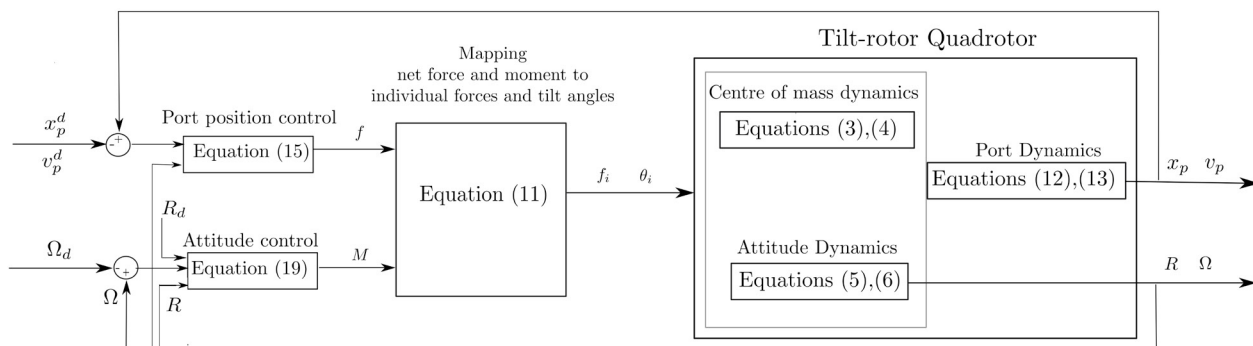
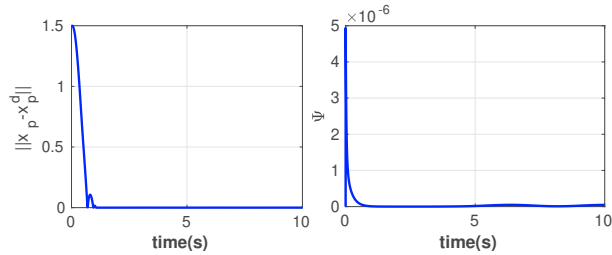


Fig. 2. Block diagram of the proposed control scheme



(a) Norm of position tracking error (b) Attitude error function error

Fig. 4. Case 1: Tracking errors

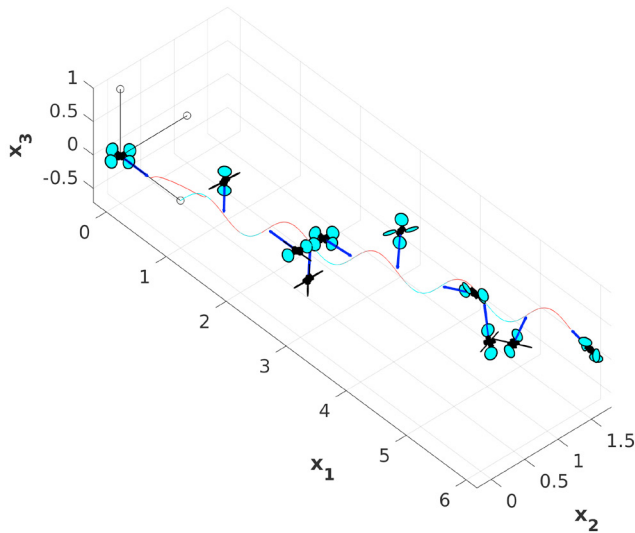
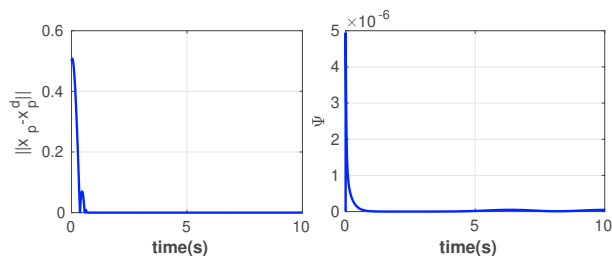


Fig. 5. Case 2: Port Trajectory

The trajectory followed by the tilt-rotor quadrotor port is shown in Fig. 3. The attitude error function, Fig. 4b, and the norm of the port position error, Fig. 4a, are presented. It can be deduced from these figures that both the attitude tracking error and port tracking error reduce to the desired values.



(a) Norm of position tracking error (b) Attitude error function error

Fig. 6. Case 2: Tracking errors

Similar to the previous case, the trajectory followed by the tilt-rotor port and the corresponding translational and rotational errors respectively are illustrated in Fig. 5 and Fig. 6. The trajectory tracking capabilities can be verified from the port position error plots.

From the presented results, we can observe that the tilt-rotor quadcopter employing the proposed controller can

track a port trajectory while following an attitude profile. This can be useful in many applications incorporating vision based functions where it is critical that the camera mounted on the device's body should either remain unaffected or follow an independent attitude profile while tracing a desired translational trajectory.

## 5. CONCLUSIONS

In this paper, the control of a port mounted on the tilt-rotor quadcopter has been addressed. We have proposed a sliding mode controller to track desired port position and velocity trajectories. The proposed control scheme enables the independent tracking of port and attitude trajectories. We have demonstrated the proposed trajectory tracking scheme for an eight-shaped trajectory using numerical simulations. The port trajectory tracking incorporating the constraints on the propeller tilt angles is an interesting area for future research. This study can be extended by including practical constraints on tilt-rotor flight, such as the influence of disturbances, actuator limitations, and modeling uncertainties.

## REFERENCES

- Alkamachi, A. and Erçelebi, E. (2019). A proportional derivative sliding mode control for an overactuated quadcopter. *Proceedings of the Institution of Mechanical Engineers, Part G: Journal of Aerospace Engineering*, 233(4), 1354–1363. doi:10.1177/0954410017751739.
- Chaturvedi, N.A., Sanyal, A.K., and McClamroch, N.H. (2011). Rigid-body attitude control. *IEEE Control Systems*, 31(3), 30–51.
- Falconi, R. and Melchiorri, C. (2012). *Dynamic model and control of an over-actuated quadrotor UAV*, volume 45. IFAC. doi:10.3182/20120905-3-HR-2030.00031. URL <http://dx.doi.org/10.3182/20120905-3-HR-2030.00031>.
- Invernizzi, D. and Lovera, M. (2017). Geometric tracking control of a quadcopter tiltrotor UAV. *IFAC-PapersOnLine*, 50(1), 11565–11570. doi:10.1016/j.ifacol.2017.08.1645. URL <https://doi.org/10.1016/j.ifacol.2017.08.1645>.
- Kumar, R., Nemati, A., Kumar, M., Sharma, R., Cohen, K., and Cazaurang, F. (2017). Tilting-rotor quadcopter for aggressive flight maneuvers using differential flatness based flight controller. In *Dynamic Systems and Control Conference*, volume 58295, V003T39A006. American Society of Mechanical Engineers.
- Lee, T., Leoky, M., and McClamroch, N.H. (2010). Geometric tracking control of a quadrotor UAV on SE(3). In *Decision and Control (CDC), 2010 49th IEEE Conference on*, 5420–5425. IEEE.
- Martin, J., Heredia, G., and Ollero, A. (2013). Control of an aerial robot with multi-link arm for assembly tasks. *2013 IEEE International Conference on Robotics and Automation*, 4916–4921. doi:10.1109/ICRA.2013.6631279.
- Nemati, A. and Kumar, M. (2014). Non-linear control of tilting-quadcopter using feedback linearization based motion control. *ASME 2014 Dynamic Systems and Control Conference, DSCC 2014*, 3(October). doi:10.1115/DSCC2014-6293.

- Nguyen, H.N., Ha, C., and Lee, D. (2015). Mechanics, control and internal dynamics of quadrotor tool operation. *Automatica*, 61, 289–301.
- Nguyen, H.n. and Lee, D. (2013). Hybrid Force / Motion Control and Internal Dynamics of Quadrotors for Tool Operation. *2013 IEEE/RSJ International Conference on Intelligent Robots and Systems*, 3458–3464. doi:10.1109/IROS.2013.6696849.
- Nikhilraj, A., Simha, H., and Priyadarshan, H. (2019). Optimal energy trajectory generation for a quadrotor uav using geometrically exact computations on  $se(3)$ . *IEEE Control Systems Letters*, 3(1), 216–221.
- Ryll, M., Bühlhoff, H.H., and Giordano, P.R. (2012). Modeling and control of a quadrotor UAV with tilting propellers. *Proceedings - IEEE International Conference on Robotics and Automation*, 4606–4613. doi:10.1109/ICRA.2012.6225129.
- Willis, J., Johnson, J., and Beard, R.W. (2020). State-Dependent LQR Control for a Tilt-Rotor UAV. *Proceedings of the American Control Conference*, 2020-July(1), 4175–4181. doi:10.23919/ACC45564.2020.9147931.
- Yang, H. and Lee, D. (2014). Dynamics and control of quadrotor with robotic manipulator. *Proceedings - IEEE International Conference on Robotics and Automation*, 5544–5549. doi:10.1109/ICRA.2014.6907674.